



# A Millimeter-Wave Planar Dual-Band Array Antenna Having Individually LHCP and RHCP Radiation Characteristics

JIAN-NAN WANG<sup>1</sup>, ZI-JUN GUO<sup>1</sup> <sup>1</sup> (Graduate Student Member, IEEE),  
AND ZHANG-CHENG HAO<sup>1,2,3</sup> <sup>1,2,3</sup> (Senior Member, IEEE)

<sup>1</sup>State Key Laboratory of Millimeter-Wave, Southeast University, Nanjing 210096, China

<sup>2</sup>Frontiers Science Center for Mobile Information Communication and Security, Southeast University, Nanjing 210096, China

<sup>3</sup>Purple Mountain Laboratories, Nanjing 211111, China

CORRESPONDING AUTHOR: Z.-C. HAO (e-mail: zchao@seu.edu.cn)

This work was supported in part by the National Natural Science Foundation of China under Grant 62131008, and in part by the Fundamental Research Funds for the Central Universities under Grant 2242022k30003.

**ABSTRACT** This article demonstrates a planar dual-band array antenna for millimeter-wave applications, which has a left-hand circular polarization and a right-hand circular polarization for two operating bands, respectively. By using aperture-fed stacked-curls, the proposed antenna can attain broad axial ratio (AR) bandwidths in both K- and Ka-bands through a single port. Meanwhile, two stacked-curls are designed to rotate in different directions for achieving orthogonal circular polarizations in two bands, respectively. An 8×8 stacked-curls array antenna is designed and manufactured for verifications. The measured 3 dB AR bandwidths are 11.59% (18.7-21 GHz) in the K-band and 9.93% (26.8-29.6 GHz) in the Ka-band, with reflection coefficient lower than -10 dB. The maximum gain in K- and Ka-bands are 18.59 dB and 18.13 dB, respectively. The proposed antenna can be used for developing compact satellite communication systems.

**INDEX TERMS** Millimeter-wave, dual-band, dual circular polarization, stacked curl, array antenna.

## I. INTRODUCTION

AT PRESENT, the millimeter-wave communication attracts much interests from industries and academics, such as the K-/Ka-band low earth orbit (LEO) satellite system. By adopting a high operating frequency band, it provides both high throughput and miniaturized antenna system [1]. Traditionally, two antennas must be used for two operation bands of the LEO satellite communication system, respectively, which inevitably requires a large system size. Therefore, the dual-band antenna, which has the left-hand circular polarization (LHCP) and the right-hand circular polarization character (RHCP) for each band, respectively, is of great significance for the LEO satellite communication system, because of its small size, high channel capacity, high isolation, and attenuation of multipath fading and polarization mismatch.

In recent years, several dual-band antennas with the CP radiation have been reported [2]–[14]. Generally, the techniques can be classified as two types, 1) using the same radiation structure, 2) using two radiation structures. The first generally uses different parts of the radiation structure [2], [3] or different working modes [4]–[6] to achieve the desired characteristics; the second usually requires two radiation-structures which can support two operation bands, respectively [7]–[14]. Generally, above mentioned works show attractive performance. However, most of them are operated at microwave frequency, and tolerate a narrow axial ratio (AR) bandwidth. Beyond that, their operation band and radiation characteristics cannot be adjusted flexibly.

This paper reports a novel millimeter-wave (mm-wave) dual-band array antenna with the LHCP and RHCP radiation

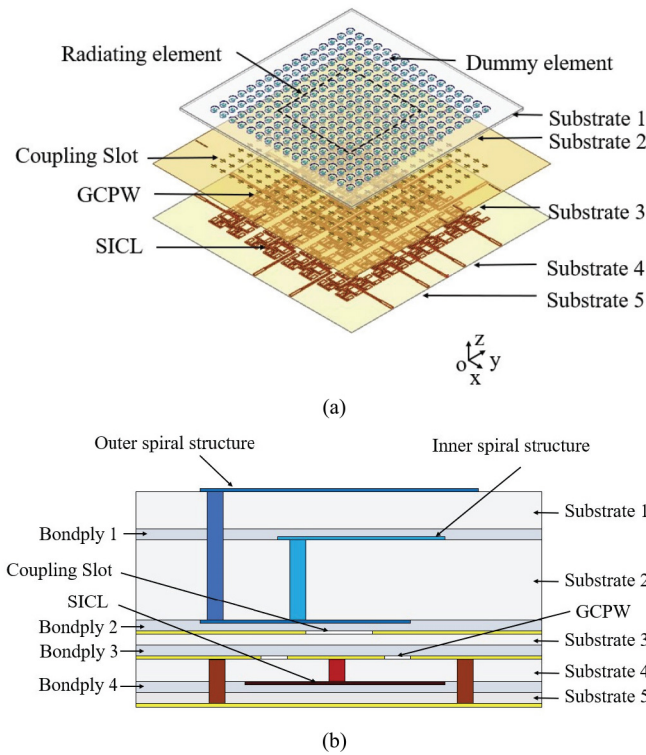


FIGURE 1. The proposed array. (a) Detailed 3-D topology. (b) Cross-sectional view.

features for each operating band, respectively. As an extension of [17], an 8x8 array having two wide AR bandwidths is demonstrated by utilizing the excellent CP radiation characteristics of stacked-curly [15]–[16], whose radiation characteristics, including operation frequency bandwidth and radiation polarization, can be designed independently. The proposed antenna is designed to support K-band applications with a left-hand circular polarization (LHCP) and Ka-band applications with a right-hand circular polarization (RHCP). Section II presents the detailed structure of the proposed antenna with its design methods, Section III verifies the design through experiments with an 8x8 prototype, and conclusions are described in Section IV.

## II. ANTENNA TOPOLOGY AND DESIGN METHOD

Fig. 1 depicts the detailed 3-D topology of the proposed array antenna. It includes five dielectric layers and four bond-plyes. The Rogers RT/duroid 5880 with loss tangent = 0.0009 and  $\epsilon_r = 2.2$  is used for the substrate 1, 2 and 3, with the thicknesses of 0.508, 1.524, and 0.254 mm, respectively. The substrate 4 and 5 have thicknesses of 0.254 mm and 0.127 mm, which use the Rogers RO4350B with  $\epsilon_r = 3.48$  and loss tangent = 0.004. The Rogers RO4450F substrate of  $\epsilon_r = 3.54$ , loss tangent = 0.004 and height = 0.1mm is adopted as bonding layers. Two stacked curls are fed by coupling in the metal-etched slot of the GCPW in substrate 3. To excite the GCPWs, a sixty-four SICL power divider

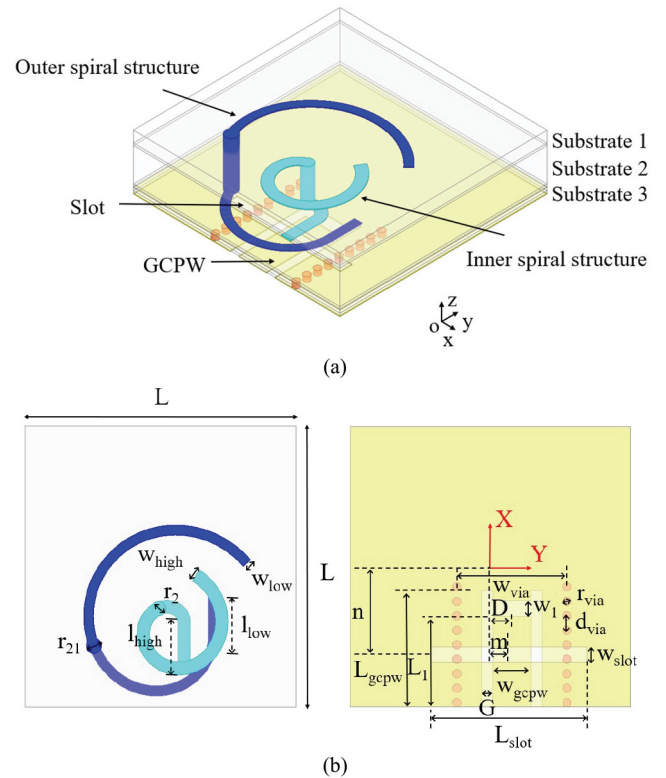


FIGURE 2. The proposed double stacked curls element. (a) 3-D view. (b) Top view.

TABLE 1. Dimensions of the designed element.

Par.	$L$	$w_{gcpw}$	$L_{gcpw}$	$G$	$w_l$	$L_1$
Val.(mm)	9.7	1.3	4.04	0.4	0.55	3.24
Par.	$w_{via}$	$r_{via}$	$d_{via}$	$w_{slot}$	$L_{slot}$	$m$
Val.(mm)	3.8	0.15	0.5	0.54	5.4	0.82
Par.	$r_2$	$w_{high}$	$l_{high}$	$r_{21}$	$w_{low}$	$l_{low}$
Val.(mm)	0.5	0.45	1.43	0.55	0.35	1.4
Par.	$D$	$n$				
Val.(mm)	0.75	3.35				
Par.	$\varphi_{st}$	$\varphi_{mid}$	$\varphi_{end}$	$\varphi_{st}$	$\varphi_{mid}$	$\varphi_{end}$
Val.(rad)	2.03	3.8	9	4.92	7.6	10.35

is designed and connected with the GCPWs through transformer structures. The dummy elements are added to reduce the grating lobe level.

### A. RADIATION ELEMENT STRUCTURE

The geometry of the proposed aperture-fed double stacked curls element is illustrated in Fig. 2 with its dimensions presented in Table 1. As is exhibited in Fig. 2, the spiral structure is composed of top spiral arm, bottom spiral arm, metallic via and straight arm. The bottom spiral arm is from  $\varphi_{st}$  to  $\varphi_{mid}$  and the top spiral arm is from  $\varphi_{mid}$  to  $\varphi_{end}$ . The top spiral arms of the inner and outer spiral structure are situated on the top surface of the substrate 2 and the top surface of the substrate 1 respectively. This spatial structure

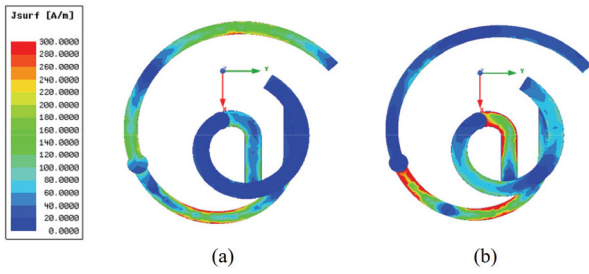


**FIGURE 3.** The electric current distribution on the stacked-curled element. (a) 18.2 GHz and (b) 28.5 GHz.

can reduce coupling between the top spiral arms. The bottom spiral arms of the inner and outer spiral structure are situated on the lower surface of the substrate 2. The straight arms connected to the corresponding bottom spiral arms are used to excite the antenna element. The stacked-curled structure is excited through the slot etched on the surface of the GCPW located on substrate 3 [15]. The rotation directions of the outer and inner spiral arms satisfy the left-hand and right-hand rules, respectively. Thus, the antenna element appears as LHCP radiation in K-band and RHCP radiation in Ka-band [17]. The size of the spiral structure is determined by the principle of Archimedes spiral [18].

The distribution of the electric current on the two stacked curls at 18.2 and 28.5 GHz are indicated in Fig. 3. It is demonstrated that the straight arms and the bottom spiral arms are located directly above the coupling slot, so the electric current exists no matter in which working band. At 18.2 GHz, there is strong electric current on the surface of the outer top spiral arm, while there is almost no electric current on the surface of the inner top spiral arm, indicating that the main radiation part at this frequency is the outer spiral structure, that is, the antenna element works with the LHCP in the K-band. Similarly, at 28.5 GHz, the main radiation part is the inner spiral structure, which works with the RHCP in the Ka-band.

Generally, the integration of two stacked-spirals operating in different frequency bands can achieve a compact footprint and improve the design flexibility. However, the AR bandwidth and the impedance bandwidth of the proposed antenna are reduced due to the interaction of those two radiation structures. Since the proposed antenna is fed by only one port, the impedance matching and the AR need to be considered simultaneously for those two structures. Thus, the operating bandwidth as well as the AR bandwidth of each stacked-spiral becomes narrower, compared with the traditional stacked-spiral antenna [15]. In addition, although the isolation between two stacked-spirals operating in different frequency bands cannot be directly extracted due to only one feed port excitation for the whole structure, it can be reflected by the radiation current distributions in different frequency bands in Fig. 3, where a small radiation current is observed, indicating a high band-isolation is achieved.

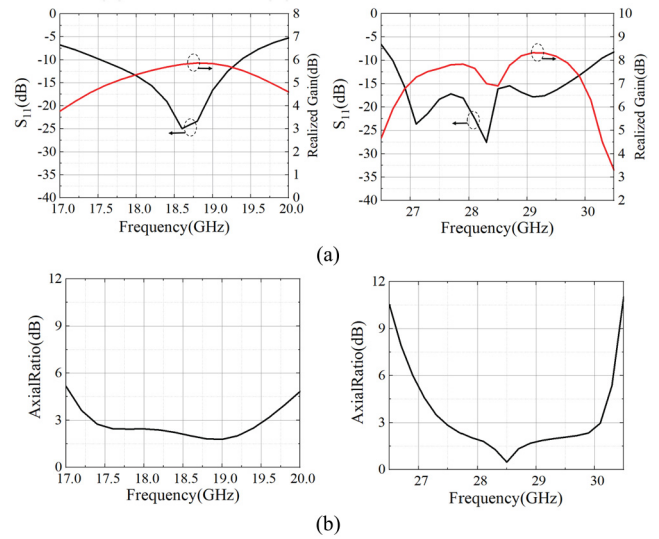


**FIGURE 4.** Simulated element performance. (a)  $S_{11}$  and gain. (b) AR.

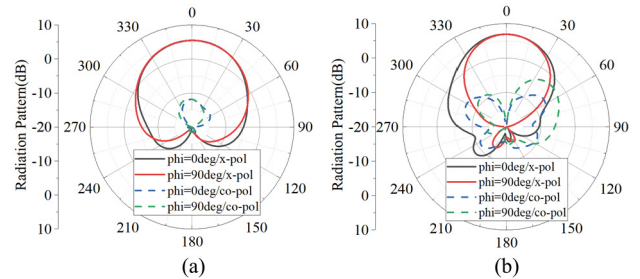


**FIGURE 5.** Simulated element radiation patterns. (a) 18.2 GHz and (b) 28.5 GHz.

Fig. 4 and Fig. 5 present the simulated performance of the proposed element, which is simulated with a periodic boundary for modelling array applications. The simulation results display that the  $-10$  dB impedance bandwidth is 10.02% (17.53-19.38 GHz) in the K-band and 12.5% (26.69-30.25 GHz) in the Ka-band. The maximum gain in the K-band is 5.86 dB, and the whole band (17-20 GHz) is within 3 dB gain bandwidth. The maximum gain in the Ka-band is 8.33 dB and the gain bandwidth of 3 dB is 12.71% (26.6-30.21 GHz). The 3 dB AR bandwidth is 12.03% (17.34-19.56 GHz) and 9.21% (27.45-30.1 GHz). It has good CP characteristics in both bands.

### B. THE $8 \times 8$ ARRAY ANTENNA

To demonstrate the array application, an  $8 \times 8$  array antenna is schemed with a broadband substrate integrated coaxial line (SICL) feeding network illustrated in Fig. 6, which is integrated with the element antenna by using a SICL-to-GCPW transformer. The design results of the 64-way SICL feed network are shown in Fig. 7. It can be seen that in the 17-30 GHz, all  $S_{11}$  are lower than  $-12$  dB. The transmission coefficients of each port are basically the same, ranging from  $-20.75$  dB to  $-23.5$  dB. In addition, in order to reduce the grating lobe level resulted by the edge effect, a few dummy

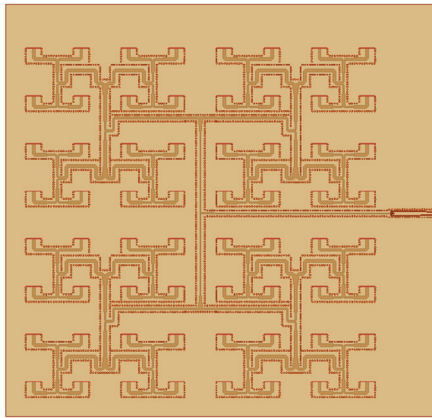


FIGURE 6. Planar structure of the designed 64-way feed network.

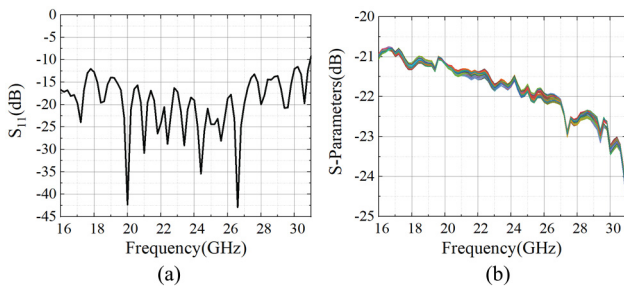


FIGURE 7. Design results of the 64-way feed network. (a) Reflection coefficient. (b) Transmission coefficient.

elements are added to the  $8 \times 8$  antenna array, which are connected with a 50 ohm resistor. The radiation performance of the designed array is presented and discussed in Section III, where the laboratorial results are compared as well.

### III. EXPERIMENTAL VERIFICATION

The  $8 \times 8$  stacked curls array antenna is fabricated and tested for verification. Fig. 8 reveals the photographs of the manufactured array and its measurement environment. The simulated and measured  $S_{11}$ , AR and realized gain are illustrated in Fig. 9. The measured  $S_{11}$  is below  $-10$  dB in 17.5-21 GHz and 26.5-30 GHz. According to the simulation results, the 3-dB AR bandwidths in K- and Ka-bands are 12.3%, from 18.52 to 20.95 GHz, and 9.91%, from 27.05 to 29.87 GHz, respectively. The measured antenna has a 3-dB AR bandwidth of 11.59% (18.7-21 GHz) in the K-band and 9.93% (26.8-29.6 GHz) in the Ka-band. The discrepancy between designed and measured results is mainly due to thickness changing of the bonding layers after several times of pressing in the fabrication. The 3 dB gain bandwidths of the measured antenna are 17.5-21 GHz and 26.5-30 GHz, and its maximum gain are 18.59 dB and 18.13 dB, respectively. The measured radiation patterns of the array antenna in the  $xoz$  and  $yoZ$  planes are presented in Fig. 10 and Fig. 11, where a sidelobe lower than  $-10$  dB is achieved for the two operation bands. It should be mentioned that the relatively large sidelobe level is resulted by

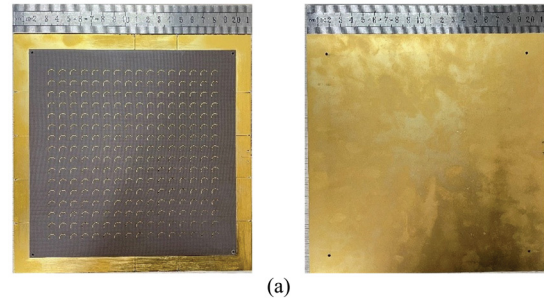


FIGURE 8. (a) Photographs of the fabricated array antenna and (b) measurement setup.

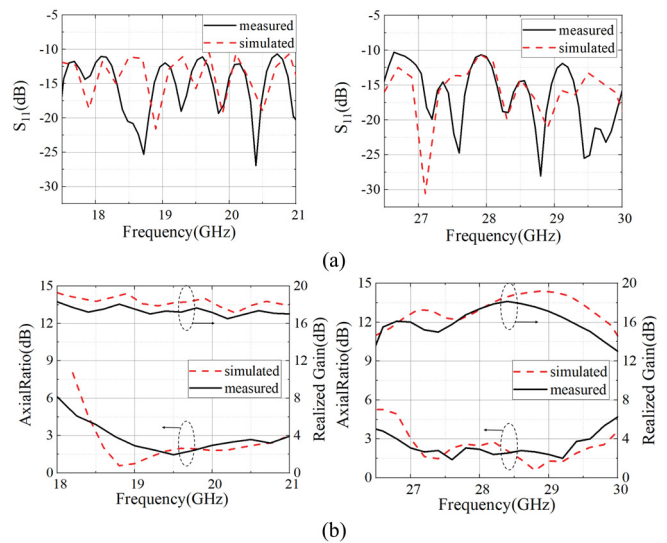
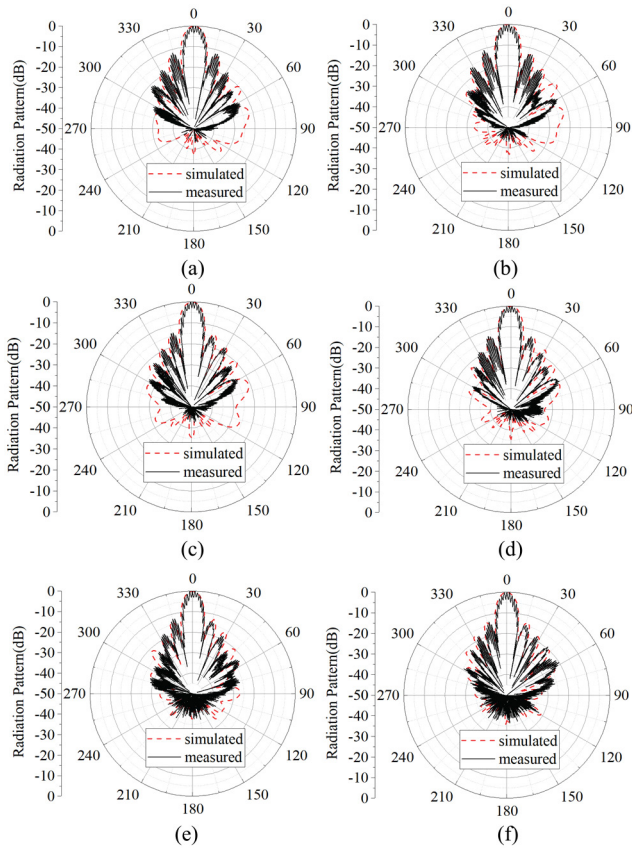


FIGURE 9. Simulated and measured performance of the array antenna. (a)  $S_{11}$  and (b) AR and realized gain.

the relatively large element, as well as the relatively large element-space. Since the Ka-band stacked-spiral is integrated inside the K-band stacked-spiral with a double-layer topology, the K-band stacked-spiral needs to be designed with a relatively large size to leave enough rooms for the Ka-band stacked-spiral. That requires a relatively large element-space in the design of the proposed array. To reduce the size of the radiation element, the element may be designed with a multiple-layer technology such as the low-temperature cofired ceramic (LTCC) technology, in which the stacked-spiral can be designed on tens of substrates. That is helpful





**FIGURE 10.** Measured radiation patterns compared with design results. (a) *xoz* plane and (b) *yoz* plane at 19 GHz. (c) *xoz* plane and (d) *yoz* plane at 20 GHz. (e) *xoz* plane and (f) *yoz* plane at 21 GHz.

**TABLE 2.** Compare of relative dual-band dual CP arrays.

Ref.	scale	Freq. (GHz)	ARBW (%)	Peak Gain (dBic)	Single feed
[3]	4×4	8.3	3	16.1	Yes
		14.5	4.1	15.2	
[6]	2×2	2.53	0.67	10.8	Yes
		3.59	0.6	12.5	
[13]	4×4	7.5	3.97	14.5	No
		8.1	4.55	15	
[14]	4×4	12.1	1.5	17.45	Yes
		17.4	1.5	18.26	
<b>This work</b>	<b>8×8</b>	<b>19.8</b>	<b>11.59</b>	<b>18.59</b>	<b>Yes</b>
		<b>28.2</b>	<b>9.93</b>	<b>18.13</b>	

to reduce the element-space of the array, as well as the sidelobe level.

Table 2 compares the proposed array antenna with some relative dual-band dual CP array antennas. By using a single layered hybrid patch, a high radiation efficiency is achieved for both two operating bands in [4], which, however, has a narrow AR bandwidth. In addition, to obtain a good matching for the hybrid patch, a diplexer is required for each element in theory. Compared with the dual-band radiation patches on the single-layered or multiple-layered substrate [3], [6], [13], [14], the proposed antenna adopts

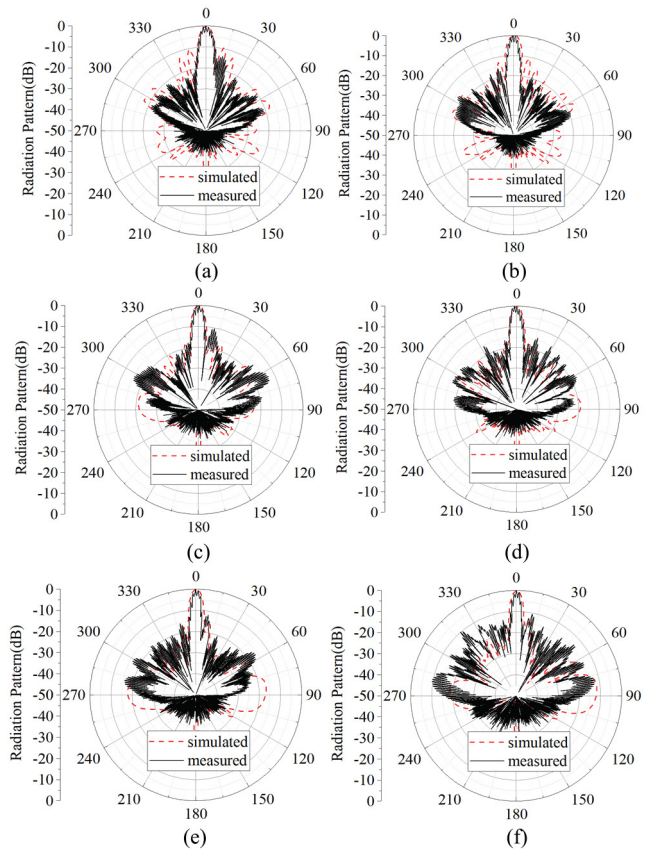


**FIGURE 11.** Measured radiation patterns compared with design results. (a) *xoz* plane and (b) *yoz* plane at 27 GHz. (c) *xoz* plane and (d) *yoz* plane at 28.3 GHz. (e) *xoz* plane and (f) *yoz* plane at 29.6 GHz.

two stacked-spirals as the basic radiation structure, which can provide much wider AR bandwidth than relative works in the Table 2, as shown in [15], [16]. Since two stacked-spirals are coupled individually with the feed line through the coupling slot, respectively, a good impedance matching can be obtained for each operating frequency band by mainly adjusting the corresponding stacked-spiral. It should be mentioned that the radiation efficiency is lower than that of the compared works in Table 2. That is resulted by a few reasons as following: 1) the proposed antenna has the highest operating frequency. At the operating frequency, the dielectric and metallic loss are much larger than that of the lower frequency. 2) in order to feed the hybrid stacked-spirals and obtain a planar topology, a relatively complicated feed network has to be adopted for the proposed array, which includes the SICL lines, the SICL-to-GCPW transition, the GCPWs, and coupling slots. This feed network leads to a higher insertion loss than that of the single-layered feed network. Nevertheless, a good radiation gain around 18.0 dBic is achieved for the two operating frequency bands of the measured prototype.

#### IV. CONCLUSION

In this article, a planar millimeter-wave dual-band and dual CP array antenna is proposed based on the aperture-fed double stacked-curles. The design principle has been discussed in

detail, and confirmed through simulations and experiments. The measured results indicated that the  $S_{11}$  is below  $-10$  dB in 17.5–21 GHz and 26.5–30 GHz, the 3-dB AR bandwidth is 11.59% in K-band and 9.93% in Ka-band, with a maximum gain of 18.59 dB and 18.13 dB, respectively. The proposed antenna can be adopted for developing compact LEO satellite communication system.

## REFERENCES

- [1] H. Fenech, S. Amos, A. Tomatis, and V. Soumpholphakdy, "High throughput satellite systems: An analytical approach," *IEEE Trans. Aerosp. Electron. Syst.*, vol. 51, no. 1, pp. 192–202, Jan. 2015.
- [2] K. Kumar, S. Dwari, and M. K. Mandal, "Dual-band dual-sense circularly polarized substrate integrated waveguide antenna," *IEEE Antennas Wireless Propag. Lett.*, vol. 17, no. 3, pp. 521–524, Mar. 2018.
- [3] J. Zhu, Y. Yang, S. Li, S. Liao, and Q. Xue, "Dual-band dual circularly polarized antenna array using FSS-integrated polarization rotation AMC ground for vehicle satellite communications," *IEEE Trans. Veh. Technol.*, vol. 68, no. 11, pp. 10742–10751, Nov. 2019.
- [4] Y. M. Pan, S. Y. Zheng, and W. Li, "Dual-band and dual-sense omnidirectional circularly polarized antenna," *IEEE Antennas Wireless Propag. Lett.*, vol. 13, pp. 706–709, 2014.
- [5] D. Yu, S. Gong, Y. Wan, and W. Chen, "Omnidirectional dual-band dual circularly polarized microstrip antenna using  $TM_{01}$  and  $TM_{02}$  modes," *IEEE Antennas Wireless Propag. Lett.*, vol. 13, pp. 1104–1107, 2014.
- [6] J. Zhang, L. Zhu, N. Liu, and W. Wu, "Dual-band and dual-circularly polarized single-layer microstrip array based on multiresonant modes," *IEEE Trans. Antennas Propag.*, vol. 65, no. 3, pp. 1428–1433, Mar. 2017.
- [7] Z.-X. Liang, D.-C. Yang, X.-C. Wei, and E.-P. Li, "Dual-band dual circularly polarized microstrip antenna with two eccentric rings and an arc-shaped conducting strip," *IEEE Antennas Wireless Propag. Lett.*, vol. 15, pp. 834–837, 2016.
- [8] W. Wang, C. Chen, S. Wang, and W. Wu, "Switchable dual-band dual-sense circularly polarized patch antenna implemented by dual-band phase shifter of  $\pm 90^\circ$ ," *IEEE Trans. Antennas Propag.*, vol. 69, no. 10, pp. 6912–6917, Oct. 2021.
- [9] R. K. Saini, S. Dwari, and M. K. Mandal, "CPW-fed dual-band dual-sense circularly polarized monopole antenna," *IEEE Antennas Wireless Propag. Lett.*, vol. 16, pp. 2497–2500, 2017.
- [10] Y. Chen, Y. Jiao, G. Zhao, F. Zhang, Z. Liao, and Y. Tian, "Dual-band dual-sense circularly polarized slot antenna with a C-shaped grounded strip," *IEEE Antennas Wireless Propag. Lett.*, vol. 10, pp. 915–918, 2011.
- [11] Y. Liu, Z. Yue, Y. Jia, Y. Xu, and Q. Xue, "Dual-band dual-circularly polarized antenna array with printed ridge gap waveguide," *IEEE Trans. Antennas Propag.*, vol. 69, no. 8, pp. 5118–5123, Aug. 2021.
- [12] C. Chen and E. K. N. Yung, "Dual-band dual-sense circularly-polarized CPW-fed slot antenna with two spiral slots loaded," *IEEE Trans. Antennas Propag.*, vol. 57, no. 6, pp. 1829–1833, Jun. 2009.
- [13] C. Mao, Z. H. Jiang, D. H. Werner, S. S. Gao, and W. Hong, "Compact self-diplexing dual-band dual-sense circularly polarized array antenna with closely spaced operating frequencies," *IEEE Trans. Antennas Propag.*, vol. 67, no. 7, pp. 4617–4625, Jul. 2019.
- [14] J.-D. Zhang, W. Wu, and D.-G. Fang, "Dual-band and dual-circularly polarized shared-aperture array antennas with single-layer substrate," *IEEE Trans. Antennas Propag.*, vol. 64, no. 1, pp. 109–116, Jan. 2016.
- [15] Q. Wu, J. Hirokawa, J. Yin, C. Yu, H. Wang, and W. Hong, "Millimeter-wave planar broadband circularly polarized antenna array using stacked curl elements," *IEEE Trans. Antennas Propag.*, vol. 65, no. 12, pp. 7052–7062, Dec. 2017.
- [16] Z. Chen *et al.*, "Low-profile circularly polarized staircase curl antenna array with 2:1 impedance and 50% AR bandwidths for 5G mmW communications," *IEEE Trans. Antennas Propag.*, vol. 70, no. 4, pp. 3082–3087, Apr. 2022.
- [17] J. Wang, Y. Cao, and Z.-C. Hao, "A millimeter-wave dual-band dual-circularly polarized element antenna," in *Proc. Int. Conf. Microw. Millimeter Wave Technol. (ICMMT)*, 2021, pp. 1–3.
- [18] H. Nakano, S. Okuzawa, K. Ohishi, H. Mimaki, and J. Yamauchi, "A curl antenna," *IEEE Trans. Antennas Propag.*, vol. 41, no. 11, pp. 1570–1575, Nov. 1993.